Available online at www.sciencedirect.com

ScienceDirect

Journal of the Chinese Medical Association 81 (2018) 1077−1087

www.jcma-online.com

Original Article

Involvement of S100A4/Mts1 and associated proteins in the protective effect of fluoxetine against MCT − Induced pulmonary hypertension in rats

Zhan-Hong Song [a], Han-Ming Wang [a], Ming Liu [a,c], Yang Bai [a], Yun Wang [a], Huai-Liang Wang [a,b,*]

[a] *Department of Clinical Pharmacology, School of Pharmacy, The First Affiliated Hospital, China Medical University, Shenyang, China*
[b] *National Key Laboratory, Institute of Respiratory Diseases, The First Affiliated Hospital, China Medical University, Shenyang, China*
[c] *Institute of Cardiovascular Diseases, The First Affiliated Hospital, China Medical University, Shenyang, China*

Received November 12, 2017; accepted March 11, 2018

Abstract

Background: Pulmonary arterial hypertension (PAH) is a complex pulmonary vasculature disease characterized by remodeling of the pulmonary vessels and a persistent increase in the pulmonary vascular resistance (PVR) with a poor prognosis. Serotonin increases the expression of S100A4/Mts1, which in turn stimulates the proliferation and migration of human pulmonary artery smooth muscle cells through the interaction with RAGE (receptor for advanced glycation end products) and thus S100A4/Mts1 has been implicated in the development of PAH *in vitro*. Fluoxetine, a selective serotonin re-uptake inhibitor has been shown to protect against PAH. The current study was designed to test whether S100A4 and its associated proteins connected in the development of PAH *in vivo* as well as to investigate the involvement of those proteins in the protective effect of fluoxetine against PAH.
Methods: MCT-induced PAH models were established in Wistar rats by a single intraperitoneal injection of MCT (60 mg/kg). Fluoxetine (2 and 10 mg/kg/day) was intragastrically administered once a day for 3 weeks along with controls. The detection methods followed include Hematoxylin and Eosin (H&E) staining, immunohistochemistry, western blotting and real-time reverse transcription-polymerase chain reaction (RT-PCR).
Results: MCT induced pulmonary hypertension, pulmonary vascular remodeling, and right ventricular hypertrophy significantly increased the expressions of S100A4 and RAGE in the pulmonary arteries, lungs and right ventricle (RV). Fluoxetine dose-dependently inhibited MCT-induced pulmonary arterial hypertension, pulmonary vascular remodeling, and right ventricular hypertrophy and reduced the S100A4 and RAGE. Further analysis revealed that fluoxetine alleviated both the increase of p53, MMP13, MMP2 and MMP9 and the decrease of pp53Ser15 and MDM2 in lungs and RV tissues of MCT-induced PAH rats.
Conclusion: From the present investigation it could be concluded that S100A4/Mts1 and its associated proteins are involved in the evolution of MCT-induced PAH in rats and fluoxetine inhibits MCT-induced PAH in rats mainly through S100A4/RAGE signaling axis and involved factors.

Keywords: Fluoxetine; MDM2; MMP13; MMP2; MMP9; Monocrotaline; p53; pp53 Ser15; RAGE; Remodeling; S100A4/Mts1; Serotonin transporter

1. Introduction

Pulmonary arterial hypertension (PAH) is a complex pulmonary vasculature disease characterised by an increase in the mean pulmonary arterial (PA) pressure more than 25 mmHg at rest.[1] PAH is a life-threatening and progressive disease exemplified by the remodeling of pulmonary vessels which leading to a persistent increase in pulmonary vascular resistance (PVR) and causes right ventricular (RV) failure, and a poor prognosis.[2] Although the pathogenesis of PAH remains poorly understood, vascular remodeling has been confirmed to be a crucial pathological feature of PAH, and is characterized by changes in the pulmonary vascular structures associated with medial hypertrophy and distribution of extracellular matrix (ECM).

Conflicts of interest: The authors declare that they have no conflicts of interest related to the subject matter or materials discussed in this article.

* Corresponding author. Dr. Huai-Liang Wang, Department of Clinical Pharmacology, China Medical University, 92, The 2nd North Road, Heping District, Shenyang, 110001, China.
E-mail address: wanghuailiangds@126.com (H.-L. Wang).

https://doi.org/10.1016/j.jcma.2018.03.013

Serotonin (5-HT, 5-hydroxytryptamine) has been involved in the pathological process of PAH both clinically and experimentally.[3,4] Serotonin influences on the pulmonary vasculature through both serotonin transporter (SERT) and the serotonin receptors.[5] Serotonin initiates a sustained increase in the pulmonary vascular resistance (PVR) by vasoconstriction and pulmonary vascular structural remodeling associated with smooth muscle cell proliferation[6] and by the destruction of extracellular matrix.[7] Selective serotonin reuptake inhibitors (SSRIs) hinder the accumulation of extracellular serotonin and decrease the activation of serotonin receptors via blockade of SERT.[4] Fluoxetine is a highly selective 5-hydroxytryptamine transporter (5-HTT) inhibitor and as a selective serotonin uptake inhibitor it has shown protection against the proliferation of PASMCs[8] and pulmonary vascular remodeling in medial wall thickness via blocking SERT in monocrotaline (MCT)-induced pulmonary hypertensive rats.[7,9]

Recently, S100A4/Mts1 and its associated proteins have been found to be linked with pulmonary hypertension. Serotonin is involved in the synthesis and release of S100A4/Mts1,[10] and their related proteins which initiate the vascular cell migration, proliferation[10,11] and the production of matrix metalloproteinases (MMPs) in various cells through the interactions with the receptor for advanced glycation end-products (RAGE).[12] In this study, "S100A4/Mts1 and its associated proteins" have been found to be the factors involved both in inducing the proliferation of vascular cell and remodeling extracellular matrix through binding with RAGE.

S100A4/Mts1, a member of the family of S100 proteins, is an 11 kDa small dimeric EF-hand Ca^{2+}-binding protein.[13,14] It shows no enzymatic activity but exerts its biological function via the interaction with and modulating the function of target proteins from intracellular, extracellular or in both the compartments. The cell response to S100A4/Mts1 is receptor-mediated, such as RAGE on various cell types. S100A4/Mts1 has been involved in the pathogenesis of PAH both in human and in the experimental animals.[15,16]

The RAGE is a transmembrane receptor that belongs to the immunoglobulin superfamily of receptors which interacts with different ligands.[17] It is expressed at a low basal level on different healthy cell types. The RAGE was identified as a cell surface receptor for S100/Calgranulins and the key involvement of RAGE in pulmonary hypertension was based on the evidence through different scientific studies. The effect of RAGE on human pulmonary artery smooth muscle cells (hPASMCs) taken from idiopathic pulmonary arterial hypertension (iPAH) patients and in *in vivo* animal models of monocrotaline- and Sugen-induced PAH was characterized.[17,18] From these studies, the interaction with RAGE which influenced S100A4/Mts1 and its related proteins resulting in PAH has been proved.

S100A4/Mts1 interacts with tumor suppressor protein p53 to trigger its degradation by the proteasome, which promotes cell proliferation in the nucleus.[19] MDM2 (mouse double minute 2, Hdm2 in humans) is a key regulator of p53 and controls the protein levels of p53.[20] MDM2 and p53 are part of a negative feedback loop in which p53 transcriptionally induces MDM2, which in turn inactivates p53.[21] Phosphorylation at multiple sites is the main posttranslational modification of p53, which results in the stabilization of p53 through directly disrupting the function of MDM2, then leading to the transactivation of p53. It has been indicated that the phosphorylation of p53 at Ser15 (pp53Ser15) promotes the stabilization of p53 and induces the accumulation of p53 protein.[22] Moreover, the phosphorylation of p53 at Ser15 increases the transcriptional activity of p53.[23,24] S100A4/Mts1 plays a crucial role in the remodeling of extracellular matrix (ECM) by regulating the expression of matrix metalloproteinases (MMPs).[25,26] MMPs play an important role in the reconstruction of vascular structure in PAH.

It is necessary to check that S100A4/Mts1 induces both the proliferation of vascular cell through testing p53, MDM2 and pp53Ser15 and remodeling extracellular matrix by detecting MMP2, MMP9 and MMP13, through binding with RAGE. At present it remains uncertain that whether S100A4/Mts1 is involved in the protective effect of fluoxetine against pulmonary hypertension *in vivo*. Therefore, the purpose of this study is to investigate the effects of fluoxetine on S100A4/Mts1 and its related proteins against PAH in MCT-induced pulmonary hypertensive rats.

2. Methods

2.1. Animal models of PH and experimental procedure

The animals were taken care of in accordance with Guide to the Care and Use of Experimental Animals (Vol. 1, 2nd ed., 1993, and Vol. 2, 1984, available from the Canadian Council on Animal Care (CCAC), 190 O'Connor St, Suite 800, Ottawa, ON K2P 2R3, Canada, or in the website: www.ccac.ca).

All the animals involved were approved by the Institutional Animal Care and Use Committee of China Medical University. Experiments were performed on male Wistar rats (180 ± 10 g) from the Animal Resource Center, China Medical University (certificate number: Liaoning 034). Sixty male Wistar rats were randomly assigned into four groups (n = 15 each): control (CONT), monocrotaline (MCT), MCT + fluoxetine at 2 mg/kg (MCT + F_2), and MCT + fluoxetine at 10 mg/kg (MCT + F_{10}). The MCT group and two fluoxetine-treated groups were injected intraperitoneally (ip) with a single dose (60 mg/kg) of MCT (Sigma−Aldrich, St Louis, MO, USA) to induce PH. Meanwhile, CONT group received the same volume of ethanol solution and physiological saline (0.9%) (1:4).

Fluoxetine dose-dependently inhibited MCT-induced pulmonary arterial hypertension, vascular cell proliferation and remodeling of extracellular matrix.[7,9] Fluoxetine (Cadila Pharmaceuticals Limited, Ankleshwar, India) was dissolved in distilled water. At the beginning day of MCT injection, two groups of fluoxetine-treatment rats were administered by gavage once daily with 2 mg/kg and 10 mg/kg of fluoxetine, where the groups of control and MCT rats were treated by gavage with an equal volume of vehicle (distilled water) every day for 21 days. The rats were housed in a controlled environment under a 12 h/12 h light−dark cycle at a controlled

temperature of 20 ± 2 °C and humidity (50–70%) with access to food and water *ad* libitum throughout the experimental period of 21 days.

2.2. Assessment of PAH

On Day 22, the experimental rats were anesthetized with an intraperitoneal injection of 3% sodium pentobarbital (45 mg/kg). The hemodynamic parameters were measured by following the method as previously described[18] using PV-1 polyvinyl tubes and PE-50 tubes. In brief, at first the right jugular vein and right carotid artery were isolated. Then, the pulmonary arterial pressure was measured with a polyvinyl (PV-1) catheter which was inserted into the pulmonary artery via the right jugular vein, and a polyethylene (PE-50) catheter was intubated into the right carotid artery to directly measure the systemic blood pressure. Both PV-1 and PE-50 tubes were filled with saline containing 1% heparin before catheterization. The data of pulmonary arterial pressure and systemic blood pressure were recorded with a Polygraph (Nihon Kohden RM-6000, Japan). Following this, the rats were killed with an overdose of sodium pentobarbital and the hearts were rapidly removed from the chest. Right ventricle (RV) wall was separated from left ventricle (LV) and septum (Sep), and then the wet weights of right ventricle (RV) and left ventricle plus septum (LV + S) were measured. The ratio of weight of RV to the weight of left ventricle plus septum [RV/(LV + S)] was calculated as an index of RV hypertrophy (RVH).

2.3. Hematoxylin and eosin (H&E) staining

To examine the histopathological changes of pulmonary blood vessels, hematoxylin and eosin staining (H&E) was performed as previously described. Briefly, the right lower lung tissue was perfused with physiological saline and fixed with 4% paraformaldehyde for 24 h, and was then embedded in paraffin. Paraffin-embedded lung samples were cut into a thickness of 5 μm by microtome and mounted on clean glass slides. After staining with H&E, the sections were observed under optical microscopy and analyzed by Metamorphy/BX41 (UIC/OLYMPUS, USA/JAP). Three rats from each group were studied and at least 2 slides for every individual were evaluated. Under low power, the resistant pulmonary arteries (50–200 mm) were randomly chosen and analyzed to measure the medial wall thickness. Pulmonary arteries (PA) remodeling was determined with the percentage of medial wall thickness. Medial wall thickness of pulmonary arteries was calculated by using the following equation:

$$\text{Medial wall thickness}\ (\%) = \frac{\text{External diameter} - \text{Internal diameter}}{\text{External diameter}} \times 100\%$$

2.4. Immunohistochemical staining

Immunohistochemical (IHC) reaction was performed with an Ultra Sensitive TM SP KIT and diaminobenzidine (DAB) Staining Kit (Maxin Biotech Inc., Fuzhou, China). As previously described, briefly the sections were in turn deparaffinized, rehydrated, renovated, eliminated with endogenous peroxidase activity and blocked. Then, the sections were individually incubated overnight at 4 °C with rabbit polyclonal anti-S100A4 antibody (1:50; Abcam, UK) and mouse monoclonal anti-MDM2 antibody (1:50; Beijing Biosynthesis Biotechnology, China). After incubation with diluted biotinylated secondary antibody, the sections were incubated with streptavidin-biotin-horseradish peroxidase complex. Later, several rinsing was carried out with PBS and diaminobenzidine (DAB) was added to the sections for several seconds to 2 min to achieve a complete washing which was followed by counterstaining with hematoxylin. Lastly, the sections were dehydrated, cleared and were sealed by coverslips with permount. The slides were examined with a computer-assisted microscope (Olympus) and images were taken with a BX51/MetaMorphic microscope (Olympus). The average values of optical density data indicated the protein content indirectly.

2.5. Real-time reverse transcription polymerase chain reaction (RT-PCR)

The mRNA levels of MDM2 and glyceraldehyde-3-phosphate dehydrogenase (GAPDH) were analyzed by using quantitative real-time RT-PCR. As previously described, briefly, total RNA was isolated from the homogenates of lung tissues of rats using Trizol Reagent (Takara Biotechnology, China) according to the manufacturer's instructions. Briefly, 1 ml of Trizol reagent was added to the lung tissue and homogenized by a polytron homogenizer (Kinematical AG, Lucerne, Switzerland) by blending with 200 μL of chloroform and the solution was then vigorously mixed. Then, the sample was centrifuged for 15 min at 4 °C, and the supernatant was separated. After precipitation and washing, the purified RNA was extracted. The quantity and quality of RNA were determined by NanoDrop (PeqLab, Erlangen, Germany). Equal mounts (2 μg) of RNA from each sample were used as templates for the reaction of reverse transcription to generate cDNA using PrimeScipt RT reagent Kit (Takara Biotechnology, China) for 15 min at 37 °C, and for 5 s at 85 °C. Real-time PCR was carried out on a LightCycler (Roche Diagnostics, Penzberg, Germany). The reaction mixture of a total volume of 20 μl contained 10 μl SYBR® Premix Ex Taq II (2×) having TaKaRa Ex Taq® HS, dNTP mixture, Mg^{2+}, Tli

RNase H, SYBR® Green I (Takara Biotechnology, China), 2 μl of cDNA templates, 0.8 μl of PCR Forward primer (10 mM), 0.8 μl of PCR Reverse primer (10 mM) and 6.4 μl of ddH_2O. The reaction conditions were as follows: 95 °C for 30 s to pre-incubation, 95 °C for 5 s and 60 °C for 20 s to amplification, 95 °C for 10 s and 65 °C for 10 s to melting curve, 40 °C for 30 s to cooling. The mRNA levels were corrected by the expression of GAPDH as an endogenous standard. The ΔΔCT method for relative quantification was adopted to determine the fold change in expression. The differences in the Ct values of the sample and GAPDH were calculated ($\Delta CT = CT_{Target} - CT_{GAPDH}$). It was further normalized with the control ($\Delta\Delta CT = \Delta CT - CT_{Control}$). Then, the fold change in the expression was obtained as ($2^{-\Delta\Delta CT}$) and expressed as log $2^{-\Delta\Delta CT}$. The forward and reverse sequences of the primers in quantitative PCR were synthesized (Takara Biotechnology, Dalian, China).

2.6. Western blotting

As previously described, briefly, the pulmonary artery, lung and heart tissues of frozen rat from each group were homogenized with a polytron homogenizer (Kinematica AG, Lucerne, Switzerland) in Lysis buffer (Sigma, St. Louis, MO) containing protease inhibitors to extract the protein. Equal amounts (60 μg) of proteins were loaded in each lane and then subjected to electrophoresis on a SDS-PAGE (7.5–15%) and transferred onto polyvinylidene difluoride (PVDF) membranes (Bio-Rad, Hercules, CA, USA). After blocking with non-fat dry milk (5%, w/v) for 2 h at room temperature, the membranes were incubated overnight at 4 °C with the following: primary antibodies, rabbit polyclonal anti-S100A4 antibody (1:400; Abcam, UK), rabbit polyclonal anti-RAGE antibody (1:400; Boster, China), rabbit polyclonal anti-p53 antibody (1:400; Boster, China), mouse monoclonal anti-MDM2 antibody (1:400; Beijing Biosynthesis Biotechnology, China), rabbit polyclonal anti-p-p53 antibody (1:500; Bioworld Technology, Inc, USA), rabbit polyclonal anti-MMP13 antibody (1:400; Boster, China), rabbit polyclonal anti-MMP2 antibody (1:400; Boster, China), mouse monoclonal anti-MMP9 antibody (1:500; Beijing Biosynthesis Biotechnology, China), rabbit polyclonal anti-β-actin antibody (1:3000; Santa Cruz Biotechnology, CA, USA). After washing with 1 × PBS-0.1% Tween, the membranes were individually incubated in the horseradish peroxidase conjugated secondary goat anti-mouse and anti-rabbit antibodies (Santa Cruz Biotechnology, CA, USA) for 2 h at room temperature. The detection of proteins was performed using ECL-Plus Western blotting reagents (Amersham, GE Healthcare, CT, USA) and the protein expression was analyzed by densitometry using Image Quant Software (Molecular Dynamics, Sunnyvale, CA, USA).

2.7. Statistical analysis

All the data were expressed as the mean ± SD. Statistical analysis was performed with one-way analysis of variance (ANOVA) using the Statistical Software, SPSS version 11.0 (SPSS Inc., Chicago, USA). Values of $p < 0.05$ were considered to be statistically significant.

3. Results

3.1. Hemodynamic parameters and right ventricular hypertrophy

Both mean pulmonary arterial pressure (mPAP) and RVI (%) in the MCT group were increased significantly which indicated that MCT-induced PAH models were successful. The decreasing values in the fluoxetine-treated groups were dose-dependent, which showed that the fluoxetine has an influence to prevent the development of MCT-induced PAH. No significant differences were observed in case of the mean systemic arterial pressure (mSAP) measured in all the groups (Table 1). All the above data showed that MCT induced remarkable pulmonary artery remodeling, yet, the fluoxetine prevented the change induced by MCT.

3.2. Morphometric analysis of the pulmonary arteries

Pulmonary arterial remodeling has been shown by the representative photomicrographs of pulmonary arteries stained with H&E from the control, MCT, MCT + F2 and MCT + F10 groups of rats and were measured as the percentage of medial wall thickness. The thickness of pulmonary arterial vessels medial wall increased markedly in the MCT group. As compared with other groups, the percentage of medial wall thickness in the MCT group increased from 34.4 ± 5.8% to 46.5 ± 6.3% ($p < 0.001$, MCT vs control) and

Table 1
Comparison of body weight, mSAP, mPAP, RVI in the different group.

	Control (n = 6)	MCT (n = 6)	MCT + F2 (n = 6)	MCT + F10 (n = 6)
Body weight (g)	249 ± 20	251 ± 14	255 ± 14	245 ± 13
mSAP (mmHg)	128 ± 23	114 ± 16	118 ± 11	120 ± 7
mPAP (mmHg)	16.2 ± 2.2	30 ± 3.9***	28.5 ± 4.8***	22.7 ± 2.2**##
MT (%)	34.4 ± 3.4	46.5 ± 2.6***	41.6 ± 2.8***	38.4 ± 3.6*###
RVI (%)	29.8 ± 2.8	53.3 ± 4.3***	49.8 ± 3.6***	39.6 ± 4.1***###

mSAP = mean systemic arterial pressure; mPAP = mean pulmonary arterial pressure; MT = medial wall thickness; RVI = right ventricular index. Data are expressed as mean ± SD; ***$p < 0.001$ *vs* control; **$p < 0.01$ *vs* control; *$p < 0.05$ *vs* control; ###$p < 0.001$ *vs* MCT; ##$p < 0.01$ *vs* MCT. MCT = monocrotaline; F2 = 2 mg $kg^{-1}\cdot d^{-1}$ fluoxetine; F10 = 10 mg $kg^{-1}\cdot d^{-1}$ fluoxetine.

decreased to 41.6 ± 5.8% in the MCT + F_2 group ($p < 0.001$, MCT vs MCT + F_2) and to 38.4 ± 4.4% in the MCT + F_{10} group ($p < 0.001$, MCT vs MCT + F_{10}), respectively (Fig. 1).

3.3. Expression of S100A4 and RAGE

Expressions of S100A4 and RAGE in the rat pulmonary arteries, lung and right ventricular tissues were measured by the western blotting technique.

Rat pulmonary arteries, S100A4 significantly increased in the MCT group as compared with the control group (0.76 ± 0.17 vs 1.24 ± 0.17, $p < 0.01$). Fluoxetine attenuated MCT-induced S100A4 increase in the MCT + F10 group (0.88 ± 0.14, $p < 0.05$ vs MCT). RAGE significantly increased in the MCT group as compared with the control group (0.18 ± 0.05 vs 0.59 ± 0.13, $p < 0.01$) (Fig. 2).

Rat lung, S100A4 and RAGE upregulated in the MCT group as compared with the control group (0.88 ± 0.13 vs 1.28 ± 0.15, $p < 0.01$; 0.83 ± 0.24 vs 1.42 ± 0.15, $p < 0.05$). Fluoxetine down regulated both S100A4 and RAGE in MCT + F10 group (0.95 ± 0.13, $p < 0.05$ vs MCT; 0.89 ± 0.39, $p < 0.05$ vs MCT) (Fig. 3).

S100A4 and RAGE in the right ventricle of rat increased in the MCT group as compared with the control group (0.51 ± 0.09 vs 0.89 ± 0.20, $p < 0.001$; 0.74 ± 0.18 vs 1.12 ± 0.24, $p < 0.05$) (Fig. 4).

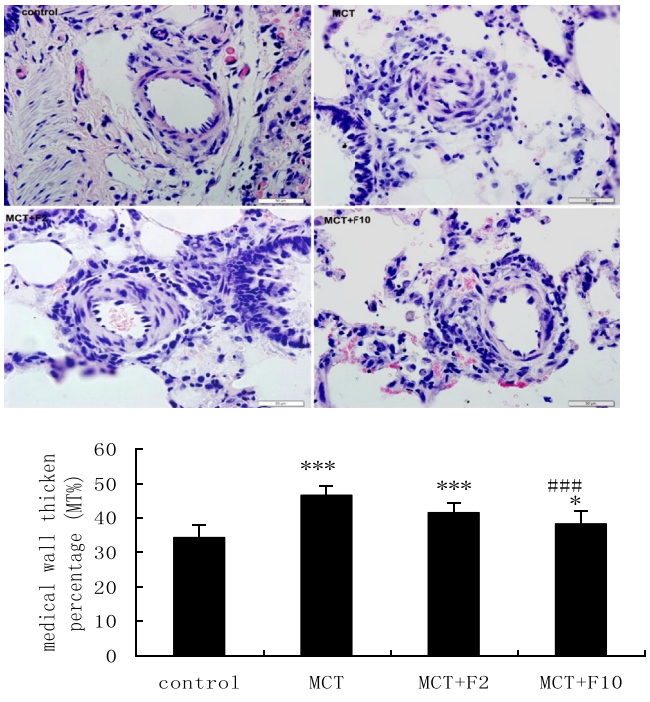

Fig. 1. Pulmonary arterial remodeling illustrated by representative photomicrographs of pulmonary arteries stained with H&E from control, MCT, MCT + F2 and MCT + F10 group of rats and pulmonary arterial remodeling measured as percentage of medial wall thickness. Data are expressed as mean ± SD (n = 6), ***$p < 0.001$ *vs* control; *$p < 0.05$ *vs* control; ###$p < 0.001$ *vs* MCT. MCT = monocrotaline; F2 = 2 mg $kg^{-1}\cdot d^{-1}$ fluoxetine; F10 = 10 mg $kg^{-1}\cdot d^{-1}$ fluoxetine.

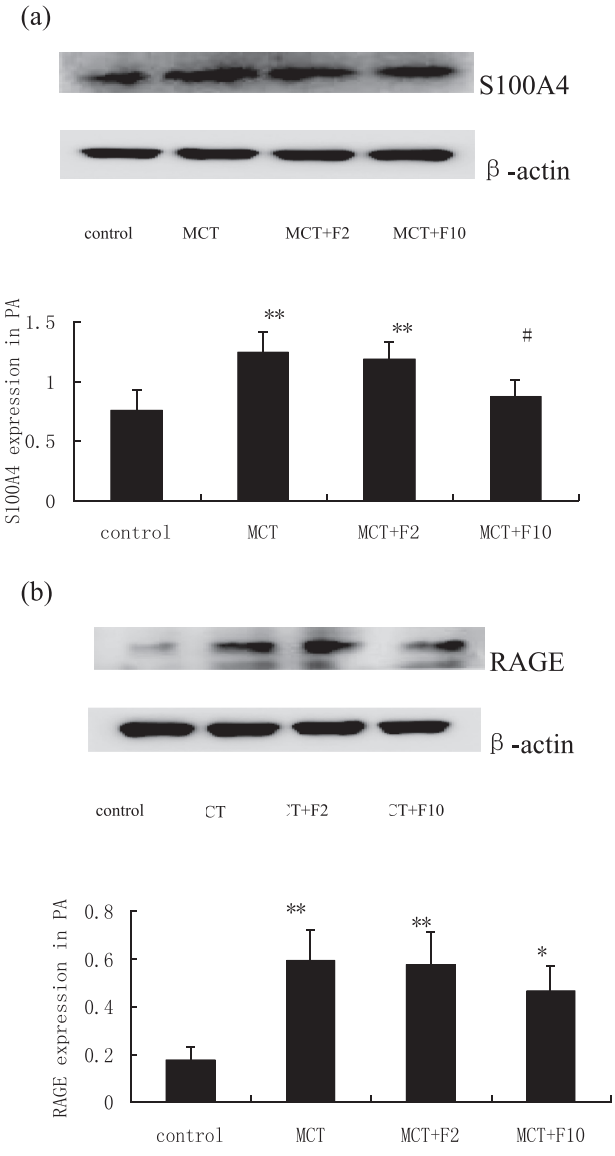

Fig. 2. Representative western blot results are displayed for the expression of S100A4 (a) and RAGE (b) in rat pulmonary arteries (PA) from control, MCT, MCT + F2 and MCT + F10 groups. Fluoxetine down regulated S100A4 and RAGE in pulmonary arteries of MCT induced PAH rat. Data are the mean ± SD (n = 3). **$p < 0.01$ *vs* control; *$p < 0.05$ *vs* control; #$p < 0.05$ *vs* MCT. MCT = monocrotaline; F2 = 2 mg $kg^{-1}\cdot d^{-1}$ fluoxetine; F10 = 10 mg $kg^{-1}\cdot d^{-1}$ fluoxetine.

Both S100A4 and RAGE expression in the rat pulmonary artery, lung and right ventricle were upregulated significantly in the MCT group as compared with the control group, whereas these levels were decreased with fluoxetine treated groups, especially in the MCT + F_{10} groups.

The slides in immunohistochemical staining reveal that S100A4 located in the medial wall of the pulmonary arteries. Meanwhile, the average optical density shows that as compared with the control group, S100A4 expression was significantly increased in the rat lungs of MCT group ($p < 0.01$, MCT vs control). The level in rat lungs was not

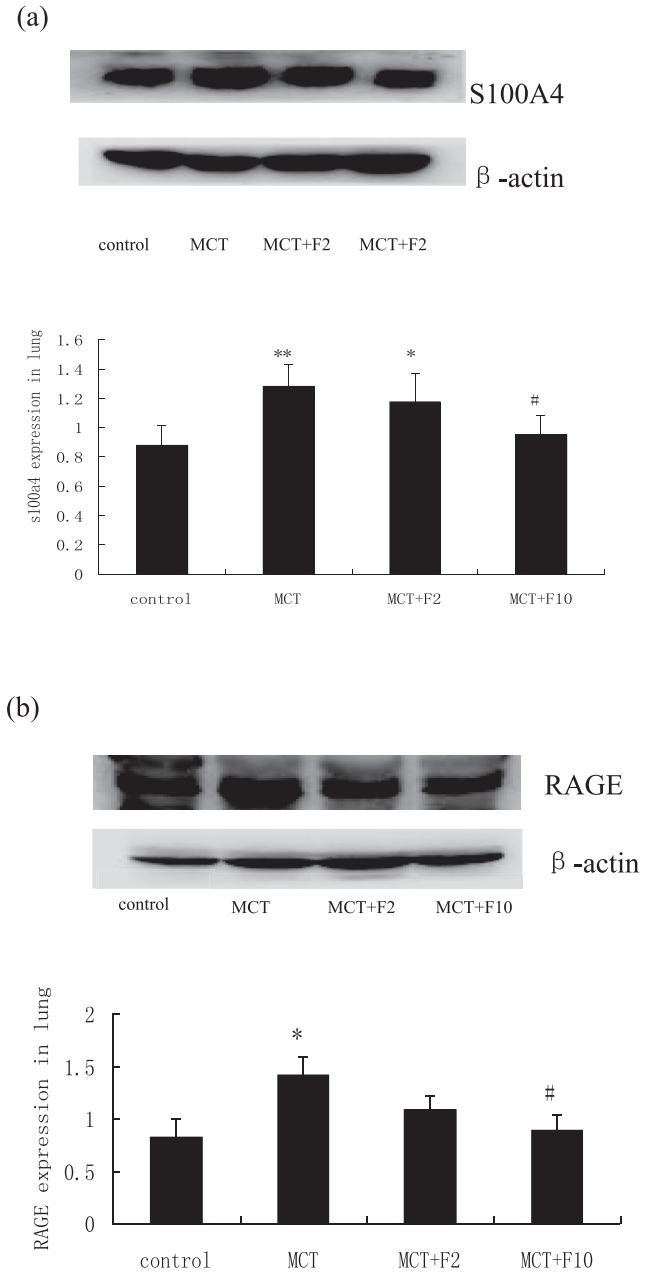

Fig. 3. Representative western blot results are displayed for the expression of S100A4 (a) and RAGE (b) in rat lungs from control, MCT, MCT + F2 and MCT + F10 groups. Fluoxetine down regulated S100A4 and RAGE in lungs of MCT induced PAH rat. Data are the mean ± SD (n = 3). $^{**}p < 0.01$ *vs* control; $^{*}p < 0.05$ *vs* control; $^{\#}p < 0.05$ *vs* MCT. MCT = monocrotaline; F2 = 2 mg $kg^{-1}\cdot d^{-1}$ fluoxetine; F10 = 10 mg $kg^{-1}\cdot d^{-1}$ fluoxetine.

markedly changed in the MCT + F_2 group as compared with the MCT group, but was significantly decreased in the MCT + F_{10} group ($p < 0.01$, MCT vs MCT + F_{10}) (Fig. 5).

These results proved that S100A4 and RAGE expression elevated markedly after MCT treatment as compared with the control group. Also, the administration of fluoxetine reduced the increased expressions in a dose-dependent manner.

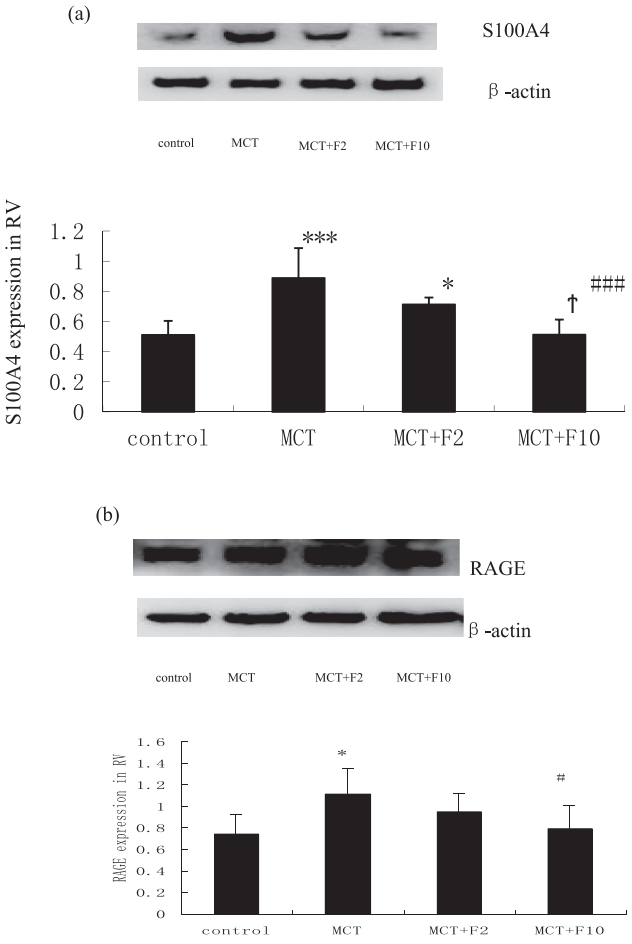

Fig. 4. Western blot analysis of S100A4 (a) and RAGE (b) in rat right ventricular (RV) from control, MCT, MCT + F2 and MCT + F10 groups. MCT increased expression of S100A4 and RAGE in rat RV, and fluoxetine down regulated the elevated S100A4 and RAGE. Data are the mean ± SD (n = 3). $^{***}p < 0.001$ *vs* control; $^{*}p < 0.05$ *vs* control; $^{\#\#\#}p < 0.001$ *vs* MCT; $^{\#}p < 0.05$ *vs* MCT. $^{\dagger}p < 0.05$ *vs* F2. MCT = monocrotaline; F2 = 2 mg $kg^{-1}\cdot d^{-1}$ fluoxetine; F10 = 10 mg $kg^{-1}\cdot d^{-1}$ fluoxetine.

3.4. Expressions of MDM2, P53, and P-P53 in rat lung

Expressions of P53 and P-P53 in rat lung tissues were measured by western blotting technique. P53 significantly increased in the MCT groups as compared with the control groups (0.66 ± 0.08 vs 1.10 ± 0.23, $p < 0.01$), whereas it decreased due to fluoxetine ($p < 0.05$, MCT vs MCT + F_{10}). P-P53 protein in the MCT groups decreased as compared with the control groups (1.31 ± 0.09 vs 0.97 ± 0.04, $p < 0.001$), and increased in the MCT + F_{10} groups ($p < 0.01$, MCT vs MCT + F_{10}) (Fig. 6).

Real-Time PCR was utilized to detect mRNA of MDM2 in the rat lung tissue. Compared with the control groups, mRNA of MDM2 decreased in the MCT groups ($p < 0.01$, MCT vs control), whereas it increased in the MCT + F_{10} groups ($p < 0.01$, MCT vs MCT + F_{10}) (Fig. 7).

The section in immunohistochemical staining shows that MDM2 is located in the medial wall of the pulmonary arteries. The average optical density was significantly decreased in the

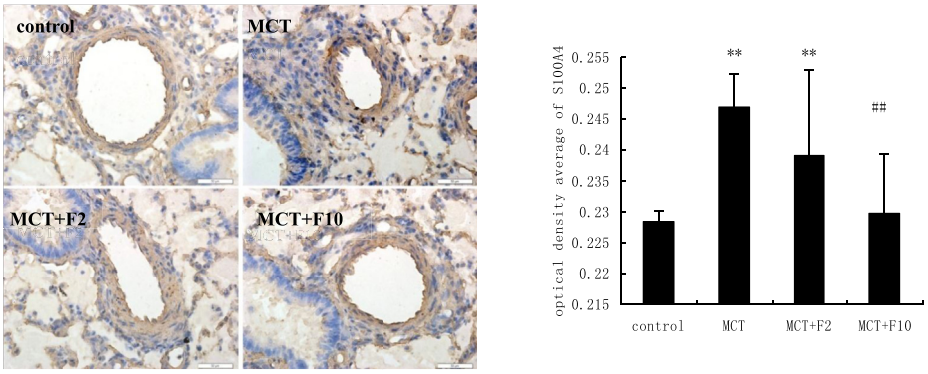

Fig. 5. S100A4 immunostaining in lungs from control, MCT, MCT + F2 and MCT + F10 group and comparison of s100a4 average comparison of s100a4 average optical density in pulmonary arteries from the four groups. S100A4 immunostaining is visible in the intima and media of pulmonary arteries. Data are the mean ± SD (n = 6). $^{**}p < 0.01$ *vs* control; $^{\#\#}p < 0.01$ *vs* MCT. MCT = monocrotaline; F2 = 2 mg $kg^{-1}\cdot d^{-1}$ fluoxetine; F10 = 10 mg kg^{-1} d^{-1} fluoxetine.

MCT group ($p < 0.01$, MCT vs control) but was significantly increased in the MCT + F_{10} group ($p < 0.01$, MCT vs MCT + F_{10}) (Fig. 8).

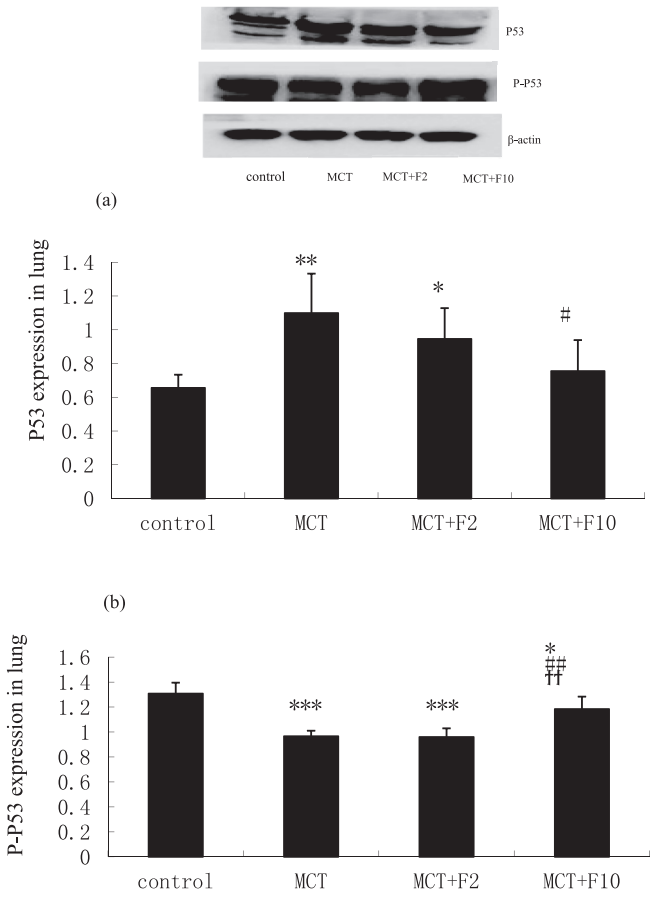

Fig. 6. Representative western blot results are displayed for the expression of P53 (a) and P-P53ser15 (b) in rat lungs from control, MCT, MCT + F2 and MCT + F10 group. Fluoxetine decreased P53 but increased P-P53ser15 in lungs of MCT induced PAH rat. Data are the mean ± SD (n = 3–4). $^{***}p < 0.001$ *vs* control; $^{**}p < 0.01$ *vs* control; $^{*}p < 0.05$ *vs* control; $^{\#\#}p < 0.01$ *vs* MCT; $^{\#}p < 0.05$ *vs* MCT; $^{\dagger\dagger}p < 0.01$ *vs* MCT + F2. MCT = monocrotaline; F2 = 2 mg $kg^{-1}\cdot d^{-1}$ fluoxetine; F10 = 10 mg $kg^{-1}\cdot d^{-1}$ fluoxetine.

3.5. Expression of MMP13 in the rat lung and right ventricle

Expressions of MMP13 in the rat lung and its right ventricular tissues were measured by western blotting technique. MMP13 both in the rat lung and right ventricular tissue were upregulated in the MCT group as compared with the control group (1.30 ± 0.34 vs 2.46 ± 0.46, $p < 0.01$; 0.56 ± 0.20 vs 0.89 ± 0.22, $p < 0.05$, respectively). Fluoxetine downregulated MMP13 in rat lung both in the MCT + F_2 groups ($p < 0.05$, MCT vs MCT + F_2) and MCT + F_{10} groups ($p < 0.05$, MCT vs MCT + F_{10}) (Figs. 9 and 10).

3.6. Expression of MMP2 and MMP9 in the right ventricular tissues of rat

Expressions of MMP2 and MMP9 in the rat right ventricular tissues were measured by western blotting technique. The level of both proteins from RV in the MCT groups were increased as compared with the control groups (0.73 ± 0.18 vs 1.13 ± 0.08, $p < 0.01$, MMP2; 0.50 ± 0.13 vs 0.82 ± 0.08, $p < 0.01$, MMP9, respectively). Fluoxetine decreased both MMP2 and MMP9 ($p < 0.05$, MCT vs MCT + F_{10}) (Figs. 11 and 12).

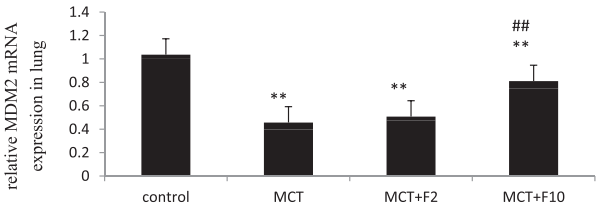

Fig. 7. Expression of MDM2 mRNA in rat lungs by a real-time polymerase chain reaction. The result of normalized CT (2ΔΔCT) analysis comparing the relative MDM2 mRNA levels of MCT, MCT + F2, MCT + F10 groups. Data are the mean ± SD (n = 4). $^{**}p < 0.01$ *vs* control; $^{\#\#}p < 0.01$ *vs* MCT. MCT = monocrotaline; F2 = 2 mg $kg^{-1}\cdot d^{-1}$ fluoxetine; F10 = 10 mg $kg^{-1}\cdot d^{-1}$ fluoxetine.

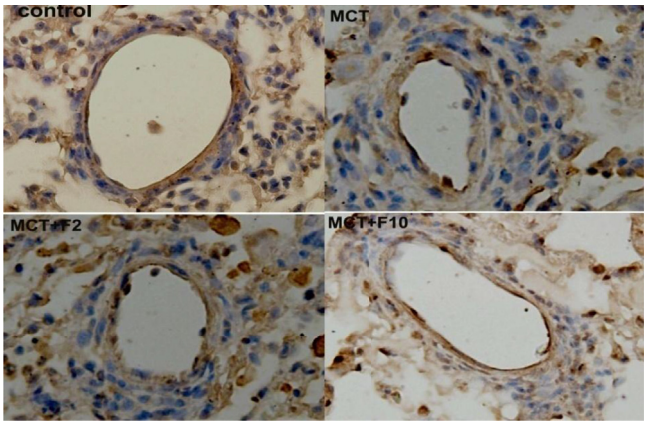

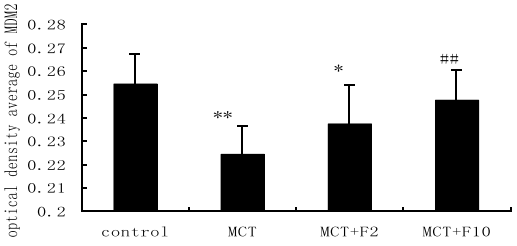

Fig. 8. MDM2 immunostaining in lungs from control, MCT, MCT + F2 and MCT + F10 group and comparison of MDM2 average optical density in pulmonary arteries from the four groups. MDM2 immunostaining is visible in the intima and media of pulmonary arteries. Data are the mean ± SD (n = 6). $^{**}p < 0.01$ *vs* control; $^{*}p < 0.05$ *vs* control; $^{\#\#}p < 0.01$ *vs* MCT. MCT = monocrotaline; F2 = 2 mg $kg^{-1}\cdot d^{-1}$ fluoxetine; F10 = 10 mg $kg^{-1}\cdot d^{-1}$ fluoxetine.

4. Discussion

The present study demonstrated that the expression levels of S100A4/Mts1 and RAGE markedly increased in the pulmonary artery, lung and right ventricle (RV); p53 of lung and RV increased but MDM2 and $pp53^{Ser15}$ decreased. Besides, both MMP2, MMP9 and MMP13 in RV and MMP13 in the lung were markedly elevated which led to structural changes in the MCT-induced PAH rats. Fluoxetine markedly inhibited the changes induced by MCT. It suggests that fluoxetine inhibits MCT-induced pulmonary vascular remodeling involved in the S100A4/RAGE axis and related factors.

To detect the effect of S100A4/Mts1 and its related proteins on fluoxetine against PAH *in vivo*, MCT-induced pulmonary hypertension in the rat was successfully confirmed via hemodynamic parameters and pathological changes.

S100A4/Mts1 and RAGE have been frequently implicated in the experimental PAH. Sustained hypoxia leads to an increase in S100A4/Mts1 and RAGE. Moreover, the experimental results suggest the potential of S100A4/Mts1 not only

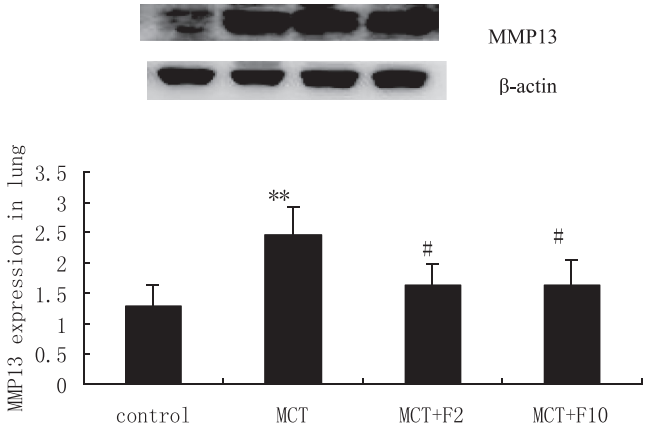

Fig. 9. Comparison of MMP13 expression in lungs of rats from control, MCT, MCT + F2 and MCT + F10 group. Data are the mean ± SD (n = 3). $^{**}p < 0.01$ *vs* control; $^{\#}p < 0.05$ *vs* MCT. MCT = monocrotaline; F2 = 2 mg $kg^{-1}\cdot d^{-1}$ fluoxetine; F10 = 10 mg $kg^{-1}\cdot d^{-1}$ fluoxetine.

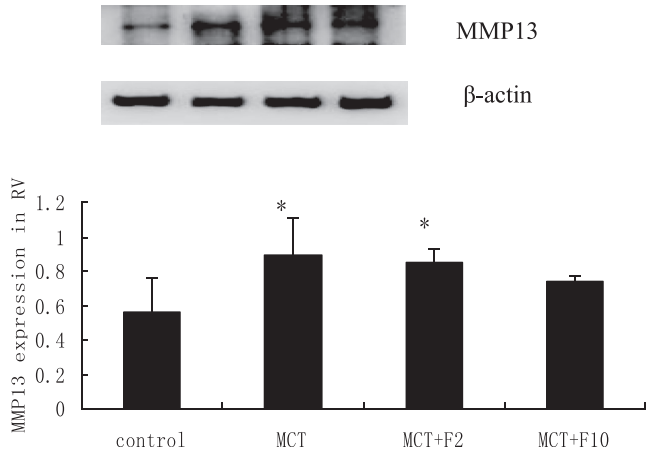

Fig. 10. Comparison of expression of MMP13 in RV of rats from control, MCT, MCT + F2 and MCT + F10 group. Data are the mean ± SD (n = 3). $^{*}p < 0.05$ *vs* control. MCT = monocrotaline; F2 = 2 mg $kg^{-1}\cdot d^{-1}$ fluoxetine; F10 = 10 mg $kg^{-1}\cdot d^{-1}$ fluoxetine.

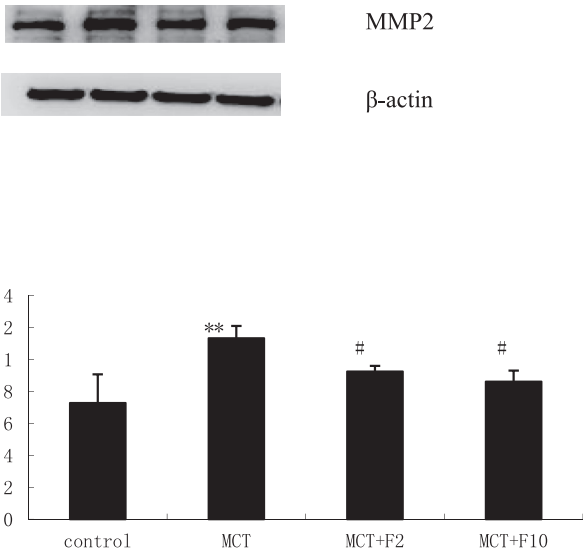

Fig. 11. Representative western blot results are displayed for the expression of MMP2 in rat RV from control, MCT, MCT + F2 and MCT + F10 group. Fluoxetine down regulated MMP2 in RV of MCT induced PAH rat. Data are the mean ± SD (n = 3). $^{**}p < 0.01$ *vs* control; $^{\#}p < 0.05$ *vs* MCT. MCT = monocrotaline; F2 = 2 mg $kg^{-1}\cdot d^{-1}$ fluoxetine; F10 = 10 mg $kg^{-1}\cdot d^{-1}$ fluoxetine.

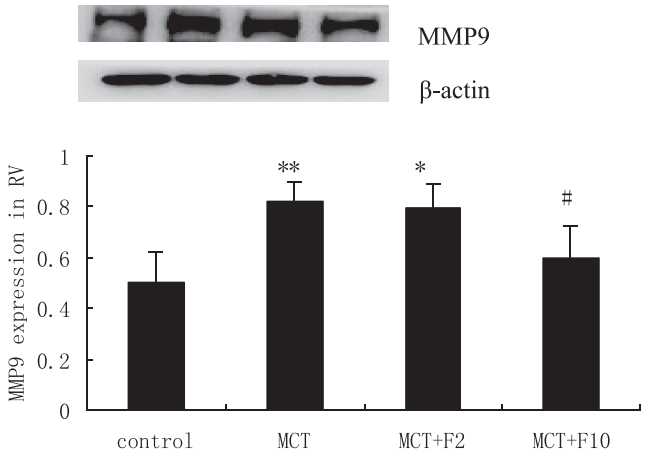

Fig. 12. Representative western blot results are displayed for the expression of MMP9 in rat RV from control, MCT, MCT + F2 and MCT + F10 group. Fluoxetine down regulated MMP9 in RV of MCT induced PAH rat. Data are the mean ± SD (n = 3). $^{**}p < 0.01$ *vs* control; $^{*}p < 0.05$ *vs* control; $^{\#}p < 0.05$ *vs* MCT. MCT = monocrotaline; F2 = 2 mg $kg^{-1}\cdot d^{-1}$ fluoxetine; F10 = 10 mg $kg^{-1}\cdot d^{-1}$ fluoxetine.

in cell motility but in the cell replication as well.[27] It is shown that S100A4/Mts1 was synthesized and released from the human pulmonary artery smooth muscle cells (hPASMCs) in response to serotonin which then acts to mediate the proliferation and migration of hPASMCs via activation of RAGE.[10] In the present study, we also observed that S100A4/Mts1 and RAGE were elevated noticeably from the pulmonary artery, lung and right ventricle (RV) in the MCT treated rats. Serotonin has been recognized to have an important influence in PAH.[5,28] Fluoxetine, as a SSRI, has been previously illustrated to be involved in the protection against PAH. The results of this study also revealed that fluoxetine inhibited MCT-induced increase of S100A4/Mts1 and RAGE in the pulmonary artery, lung and right ventricle (RV). This demonstrates that serotonin increased the expression of S100A4/Mts1 in the pulmonary artery, lung and RV thereby S100A4/Mts1 lead to pulmonary artery remodeling and RV hypertrophy via accumulated and activated RAGE in MCT-induced PAH rats. Fluoxetine decreased the abnormal changes of S100A4/Mts1 and RAGE induced by MCT through inhibiting the effect of serotonin transporter.

S100A4/Mts1, as a member of S100 calcium binding protein family was first discovered in 1989 which is also known as metastasin (Mts1), fibroblast-specific protein (FSP1), 18A2, pEL98, p9Ka, 42A, CAPL, and calvasculin.[29] S100A4/Mts1 regulates the cellular function through its interaction with other proteins. It has nuclear, cytoplasmic, and extracellular functions.[19]

It has been demonstrated that there is a functional interaction between S100A4/Mts1 and tumor suppressor protein p53.[14] The p53 expression is low and it has a short half-life in the normal cells. MDM2 (mouse double minute 2, Hdm2 in humans) is a crucial regulator of p53 and controls the protein levels of p53.[20] MDM2 negatively regulates the function of the tumor suppressor p53. MDM2 and p53 are part of a negative feedback loop in which p53 transcriptionally induces MDM2, which in turn inactivates p53.[21]

The p53 is the most frequently mutated tumor-suppressor gene. Most of the p53 mutations lead to the loss of transcription factor function and in the accumulation of dysfunctional p53 protein.[30] The p53 mutation leads to a reduction in the MDM2 transcription.[31] This may be probably due to a reduced expression of p53 target gene MDM2 and thus Mdm2 was insufficient to reduce mutant p53 as quickly as wild-type p53,[32] thereby mutant p53 often accumulates at higher levels.[33] Moreover, mutant p53 might further influence on the function of wild type p53[34–36] and p53 becomes dysfunctional through a variety of regulatory breakdowns.[37]

Phosphorylation at multiple sites is the main post-translational modification of p53, which results in the stabilization of p53 through directly disrupting the function of Hdm2 either by posttranslational modification or through regulating the interactions of Hdm2 with other cellular proteins, subsequently leading to the transactivation of p53 and increasing the transcription of various target genes.[22,38,39] It had been indicated that the phosphorylation of p53 at Ser15 ($pp53^{Ser15}$) promotes the stabilization of p53 and induces the accumulation of p53 protein.[22] Moreover, the phosphorylation of p53 at Ser15 increases the transcriptional activity of p53.[23,24]

The present study also indicates that the expressions of p53 from lung and right ventricle (RV) in the MCT-induced PAH rats increased but MDM2 and $pp53^{Ser15}$ decreased significantly. It suggests that p53 lost the function as a transcription factor and accumulated the dysfunctional p53 protein[30] which lead to a reduction in the MDM2 transcription[31] and in the disruption of p53-MDM2 feedback loop[21] in those tissues from the MCT group rats. A reduction in the $pp53^{Ser15}$ attenuated the function of p53 through promoting MDM2-mediated p53 degradation[22] and blocking the transcriptional activity of p53.[23,24]

Normally S100A4/Mts1 interacts with p53 protein to prevent cell proliferation.[19] The results of present study indicate that the effects of p53 and relevant factor (MDM2 and $pp53^{Ser15}$) were influenced in the MCT group rats resulting in the hyperproliferation of cells. This demonstrates that fluoxetine could dose-dependently attenuate those changes induced by MCT. Whether S100A4/Mts1 is directly related with p53 and interrelated factor cannot be fully explained yet the results of current study warrants for further studies.

S100A4/Mts1 plays an important role in the matrix remodeling by regulating the expression of matrix metalloproteinases (MMPs).[25,26] It has been previously indicated that extracellular S100A4/Mts1 stimulates an increased production of several MMPs, such as MMP-2 and MMP-13 via its interaction with RAGE.[40,41] MMPs are zinc-and calcium-dependent endoproteinases that play a critical role in the remodeling of extracellular matrix (ECM) by breaking down its protein components.[42,43] MMPs were usually regarded to degrade the extracellular matrix components and classified according to their substrate specificity into collagenases, gelatinases, stromelysins, matrilysins, and membrane type (MT) MMPs.[44]

The present study shows that S100A4/Mts1 increased significantly from lung and RV tissues in the MCT-induced PAH rats. Moreover, MMP2, MMP9 and MMP13 from RV and MMP13 from lung were increased significantly in the MCT-induced PAH rats. It suggests that S100A4/Mts1 promotes the production of those MMPs in lung and RV which leads to the degradation of extracellular matrix in the lung and RV of MCT-induced PAH rats. The level of RAGE in lung and RV tissues were also increased significantly in the MCT-induced PAH rats. These results suggest that the production of MMPs in lung and RV is in response to the increased S100A4/Mts1 and via its binding to RAGE. Fluoxetine reduced the elevated MMPs induced by MCT in a dose-dependent manner.

In conclusion, the present investigation for the first time confirms that S100A4/Mts1 and RAGE of PA, lung and RV tissues in PAH increased *in vivo*. The level of p53 was elevated in lung and RV tissues for the loss of function as a transcription factor and accumulation of dysfunctional protein. Then, dysfunctional p53 disrupted the feedback loop of p53-MDM2 and lead to the reduction of MDM2 in the MCT-induced PAH rats. A reduction in the phosphorylation of p53 at Ser15 ($pp53^{Ser15}$) also decreased the transcriptional activity of p53 in the MCT-induced PAH rats. The expression of MMPs in the lung and RV tissues in the MCT-induced PAH rats were increased significantly. Fluoxetine reduced those lesions to prevent the MCT-induced PAH in a dose-dependent manner. All the above pathological changes were involved in the pulmonary vascular remodeling and right ventricular hypertrophy. In conclusion, fluoxetine inhibits MCT-induced PAH in the rats operating through S100A4/RAGE signaling axis and other involved factors.

References

1. Keusch S, Turk A, Saxer S, Ehlken N, Grunig E, Ulrich S. Rehabilitation in patients with pulmonary arterial hypertension. *Swiss Med Wkly* 2017;**147**:w14462.
2. Tanaka H, Kataoka M, Isobe S, Yamamoto T, Shirakawa K, Endo J, et al. Therapeutic impact of dietary vitamin D supplementation for preventing right ventricular remodeling and improving survival in pulmonary hypertension. *PLoS One* 2017;**12**, e0180615.
3. Pleym H, Greiff G, Mjorndal T, Stenseth R, Wahba A, Spigset O. Effect of serotonin reuptake inhibitors on pulmonary hemodynamics in humans. *J Clin Med Res* 2011;**3**:230−8.
4. Gamoh S, Hisa H, Yamamoto R. 5-Hydroxytryptamine receptors as targets for drug therapies of vascular-related diseases. *Biol Pharm Bull* 2013;**36**:1410−5.
5. Marcos E, Fadel E, Sanchez O, Humbert M, Dartevelle P, Simonneau G, et al. Serotonin-induced smooth muscle hyperplasia in various forms of human pulmonary hypertension. *Circ Res* 2004;**94**:1263−70.
6. Hood KY, Mair KM, Harvey AP, Montezano AC, Touyz RM, MacLean MR. Serotonin signaling through the 5-HT 1B receptor and NADPH oxidase 1 in pulmonary arterial hypertension. *Arterioscler Thromb Vasc Biol* 2017;**37**:1361−70.
7. Li XQ, Wang HM, Yang CG, Zhang XH, Han DD, Wang HL. Fluoxetine inhibited extracellular matrix of pulmonary artery and inflammation of lungs in monocrotaline-treated rats. *Acta Pharmacol Sin* 2011;**32**:217−22.
8. Dai F, Mao Z, Xia J, Zhu S, Wu Z. Fluoxetine protects against big endothelin-1 induced anti-apoptosis by rescuing Kv1.5 channels in human pulmonary arterial smooth muscle cells. *Yonsei Med J* 2012;**53**:842−8.
9. Wang HM, Wang Y, Liu M, Bai Y, Zhang XH, Sun YX, et al. Fluoxetine inhibits monocrotaline-induced pulmonary arterial remodeling involved in inhibition of RhoA-Rho kinase and Akt signalling pathways in rats. *Can J Physiol Pharmacol* 2012;**90**:1506−15.
10. Lawrie A, Spiekerkoetter E, Martinez EC, Ambartsumian N, Sheward WJ, MacLean MR, et al. Interdependent serotonin transporter and receptor pathways regulate S100A4/Mts1, a gene associated with pulmonary vascular disease. *Circ Res* 2005;**97**:227−35.
11. Dempsie Y, Nilsen M, White K, Mair KM, Loughlin L, Ambartsumian N, et al. Development of pulmonary arterial hypertension in mice over-expressing S100A4/Mts1 is specific to females. *Respir Res* 2011;**12**:159.
12. Chaabane C, Heizmann CW, Bochaton-Piallat ML. Extracellular S100A4 induces smooth muscle cell phenotypic transition mediated by RAGE. *Biochim Biophys Acta* 2015;**1853**:2144−57.
13. Boye K, Maelandsmo GM. S100A4 and metastasis: a small actor playing many roles. *Am J Pathol* 2010;**176**:528−35.
14. Grigorian M, Andresen S, Tulchinsky E, Kriajevska M, Carlberg C, Kruse C, et al. Tumor suppressor p53 protein is a new target for the metastasis-associated Mts1/S100A4 protein: functional consequences of their interaction. *J Biol Chem* 2001;**276**:22699−708.
15. Greenway S, van Suylen RJ, Du Marchie Sarvaas G, Kwan E, Ambartsumian N, Lukanidin E, et al. S100A4/Mts1 produces murine pulmonary artery changes resembling plexogenic arteriopathy and is increased in human plexogenic arteriopathy. *Am J Pathol* 2004;**164**:253−62.
16. Kwapiszewska G, Wilhelm J, Wolff S, Laumanns I, Koenig IR, Ziegler A, et al. Expression profiling of laser-microdissected intrapulmonary arteries in hypoxia-induced pulmonary hypertension. *Respir Res* 2005;**6**:109.
17. Moser B, Megerle A, Bekos C, Janik S, Szerafin T, Birner P, et al. Local and systemic RAGE axis changes in pulmonary hypertension: CTEPH and iPAH. *PLoS One* 2014;**9**, e106440.
18. Meloche J, Courchesne A, Barrier M, Carter S, Bisserier M, Paulin R, et al. Critical role for the advanced glycation end-products receptor in pulmonary arterial hypertension etiology. *J Am Heart Assoc* 2013;**2**, e005157.
19. Xia H, Gilbertsen A, Herrera J, Racila E, Smith K, Peterson M, et al. Calcium-binding protein S100A4 confers mesenchymal progenitor cell fibrogenicity in idiopathic pulmonary fibrosis. *J Clin Invest* 2017;**127**:2586−97.
20. Hientz K, Mohr A, Bhakta-Guha D, Efferth T. The role of p53 in cancer drug resistance and targeted chemotherapy. *Oncotarget* 2017;**8**:8921−46.
21. Chauhan KM, Ramakrishnan G, Kollareddy M, Martinez LA. Characterization of cancer-associated missense mutations in MDM2. *Mol Cell Oncol* 2015;**3**, e1125986.
22. Lee JH, Kim HS, Lee SJ, Kim KT. Stabilization and activation of p53 induced by Cdk5 contributes to neuronal cell death. *J Cell Sci* 2007;**120**(Pt 13):2259−71.
23. Kojima K, Maeda A, Yoshimura M, Nishida Y, Kimura S. The pathophysiological significance of PPM1D and therapeutic targeting of PPM1D-mediated signaling by GSK2830371 in mantle cell lymphoma. *Oncotarget* 2016;**7**:69625−37.
24. Esfandiari A, Hawthorne TA, Nakjang S, Lunec J. Chemical inhibition of wild-type p53-induced phosphatase 1 (WIP1/PPM1D) by GSK2830371 potentiates the sensitivity to MDM2 inhibitors in a p53-dependent manner. *Mol Cancer Ther* 2016;**15**:379−91.
25. Miranda KJ, Loeser RF, Yammani RR. Sumoylation and nuclear translocation of S100A4 regulate IL-1beta-mediated production of matrix metalloproteinase-13. *J Biol Chem* 2010;**285**:31517−24.
26. Cao J, Geng L, Wu Q, Wang W, Chen Q, Lu L, et al. Spatiotemporal expression of matrix metalloproteinases (MMPs) is regulated by the Ca2+-signal transducer S100A4 in the pathogenesis of thoracic aortic aneurysm. *PLoS One* 2013;**8**, e70057.
27. Frid MG, Li M, Gnanasekharan M, Burke DL, Fragoso M, Strassheim D, et al. Sustained hypoxia leads to the emergence of cells with enhanced growth, migratory, and promitogenic potentials within the distal pulmonary artery wall. *Am J Physiol Lung Cell Mol Physiol* 2009;**297**:L1059−72.

28. Hervé P, Launay JM, Scrobohaci ML, Brenot F, Simonneau G, Petitpretz P, et al. Increased plasma serotonin in primary pulmonary hypertension. *Am J Med* 1995;**99**:249−54.
29. Dahlmann M, Kobelt D, Walther W, Mudduluru G, Stein U. S100A4 in cancer metastasis: Wnt signaling-driven interventions for metastasis restriction. *Cancers (Basel)* 2016;**8**. pii: E59.
30. Parrales A, Iwakuma T. Targeting oncogenic mutant p53 for cancer therapy. *Front Oncol* 2015;**5**:288.
31. Midgley CA, Lane DP. p53 protein stability in tumour cells is not determined by mutation but is dependent on Mdm2 binding. *Oncogene* 1997;**15**:1179−89.
32. Terzian T, Suh YA, Iwakuma T, Post SM, Neumann M, Lang GA, et al. The inherent instability of mutant p53 is alleviated by Mdm2 or p16INK4a loss. *Genes Dev* 2008;**22**:1337−44.
33. Wang L, Liu R, Ye P, Wong C, Chen GY, Zhou P, et al. Intracellular CD24 disrupts the ARF-NPM interaction and enables mutational and viral oncogene-mediated p53 inactivation. *Nat Commun* 2015;**6**:5909.
34. Oren M, Rotter V. Mutant p53 gain-of-function in cancer. *Cold Spring Harb Perspect Biol* 2010;**2**:a001107.
35. Petitjean A, Achatz MI, Borresen-Dale AL, Hainaut P, Olivier M. TP53 mutations in human cancers: functional selection and impact on cancer prognosis and outcomes. *Oncogene* 2007;**26**:2157−65.
36. Jones M, Lal A. MicroRNAs, wild-type and mutant p53: more questions than answers. *RNA Biol* 2012;**9**:781−91.
37. Vijayakumaran R, Tan KH, Miranda PJ, Haupt S, Haupt Y. Regulation of mutant p53 protein expression. *Front Oncol* 2015;**5**:284.
38. Shieh SY, Ikeda M, Taya Y, Prives C. DNA damage-induced phosphorylation of p53 alleviates inhibition by MDM2. *Cell* 1997;**91**: 325−34.
39. Prives C. Signaling to p53: breaking minireview the MDM2−p53 circuit. *Cell* 1998;**95**:5−8.
40. Spiekerkoetter E, Guignabert C, de Jesus Perez V, Alastalo TP, Powers JM, Wang L, et al. S100A4 and bone morphogenetic protein-2 codependently induce vascular smooth muscle cell migration via phospho-extracellular signal-regulated kinase and chloride intracellular channel 4. *Circ Res* 2009;**105**:639−47. 13 p following 647.
41. Yammani RR, Carlson CS, Bresnick AR, Loeser RF. Increase in production of matrix metalloproteinase 13 by human articular chondrocytes due to stimulation with S100A4: role of the receptor for advanced glycation end products. *Arthritis Rheum* 2006;**54**:2901−11.
42. Jaoude J, Koh Y. Matrix metalloproteinases in exercise and obesity. *Vasc Health Risk Manag* 2016;**12**:287−95.
43. Huang L, Xu Y, Cai G, Guan Z, Cai S. Downregulation of S100A4 expression by RNA interference suppresses cell growth and invasion in human colorectal cancer cells. *Oncol Rep* 2012;**27**:917−22.
44. Franco C, Patricia HR, Timo S, Claudia B, Marcela H. Matrix metalloproteinases as regulators of periodontal inflammation. *Int J Mol Sci* 2017;**18**:E440.